CIRP Annals - Manufacturing Technology xxx (2011) xxx–xxx

Contents lists available at ScienceDirect

CIRP Annals - Manufacturing Technology

journal homepage: http://ees.elsevier.com/cirp/default.asp

Identification of cutting force characteristics based on chatter experiments

G. Stepan [a,*], Z. Dombovari [a], J. Muñoa (3)[b]

[a] Department of Applied Mechanics, Budapest University of Technology and Economics, Muegyetem rkp 3, H-1111 Budapest, Hungary
[b] Dynamics and Control Department, Ideko-Danobat Group, Elgoibar, Gipuzkoa, Spain

Submitted by Laszlo Monostori (1), Budapest, Hungary.

ARTICLE INFO

Keywords:
Cutting
Force
Chatter

ABSTRACT

Cutting force coefficients exhibit strong nonlinearity as a function of chip loads, cutting speeds and material imperfections. This paper presents the connection between the sensitivity of the dynamics of regenerative cutting and the cutting force characteristic nonlinearity. The nonlinear milling process is mathematically modelled. The transitions of dynamic cutting process between the stable and unstable zones are considered and experimentally illustrated by applying wavelet transformations on the measurement data.

1. Introduction

Cutting force characteristics have important role in many aspects and especially in identifying chatter free cutting conditions. The prediction of cutting forces as a function of chip load, width of cut, speed and tool geometry is most accurately carried out by identifying cutting force coefficients from extensive, chatter free cutting tests. However, the cutting force identification tests are affected by the variations of material microstructures at different batches, dependency on cutting speeds and chip size. Due to uncertainties in the material behaviour, continuum mechanics modelling of chip formation [1,2] does not substitute the cutting experiments. Sample cutting force dependencies on chip thickness obtained from experiments and modelling approaches published in the literature are given in Fig. 1a and b to illustrate the nonlinearities in the force models.

This paper presents the connection of the nonlinear cutting force models and the dynamics of regenerative cutting. The qualitative and quantitative description of the unsafe zone is presented for the orthogonal cutting model where regenerative chatter may occur. It is shown that the constant width of the unsafe zone corresponds to the classical power law used in cutting force characteristics, while the existence of an inflexion in cutting force characteristics leads to a global maximum of the width of the unsafe zone as a function of the chip thickness.

A measurement method is introduced to identify the characteristic dependence of the width of the unsafe zone on chip thickness. The laboratory experiments are presented for full immersion milling. The critical analyses of the existing cutting force functions on chatter dynamics are presented with the support of chatter experiments.

2. Unsafe zone of stationary cutting with respect to chatter

The cutting process is called unstable if the relative vibrations between the tool and the workpiece increase for any small perturbations (like non-homogeneous workpiece material) leading to regenerative chatter; it is called stable if they disappear exponentially for small perturbations, and it is globally stable if this is the case for any large perturbations (like a hole in the workpiece material). There also exist cases when the vibrations disappear for small perturbations but they increase for large perturbations (see [3]). The idea of the so-called unsafe parameter zone refers to these cutting parameters (usually for chip width w or depth of cut a_p, see Fig. 2). The large-amplitude regenerative oscillations can be periodic, quasi-periodic (see [8]) or even chaotic (see [9,10]). In dynamic systems theory, these parameter zones are also called regions of bi-stability referring to the fact that the dynamic system has two stable solutions, the 'desired' stationary cutting and the 'undesired' chatter that leaves poor cut surface behind.

The two dynamically stable motions are separated by an unstable periodic motion, the existence of which was already recognized by Tobias in 1984 and referred to as 'finite amplitude instability' [3]. The unsafe zone is just that cutting parameter domain where this unstable periodic motion – "ghost vibration" – exists (see UZ in Fig. 2b). Although the experimental identification of this unstable periodic motion is practically impossible, the unsafe parameter zone can be detected experimentally where hysteresis is observed during the appearance/disappearance of chatter for increasing/decreasing chip width (trace blue path in Fig. 2b), or analytically by means of the parabola estimation calculated from the Hopf bifurcation (see thin black line in Fig. 2b).

The analytical estimation of the unsafe zone was derived in [11] for orthogonal cutting. The nonlinear equation of motion of the single degree-of-freedom (DoF) mechanical model of regenerative

* Corresponding author.

0007-8506/$ – see front matter © 2011 CIRP.
doi:10.1016/j.cirp.2011.03.100

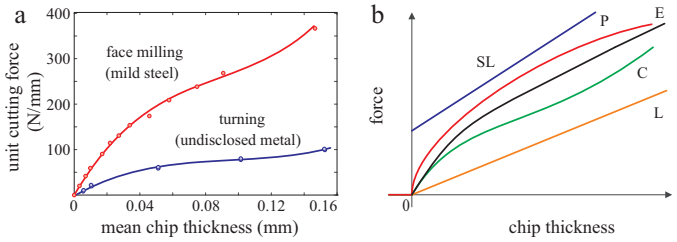

Fig. 1. (a) Measured cutting force characteristics: red [3] and blue [4]. (b) The L – linear [5], the P – power [6], the SL – shifted linear [7], the E – exponential [4] and the C – cubic polynomial [3] approximations of cutting force characteristics.

machine tool vibrations can be simplified to the form

$$\ddot{x} + 2\zeta\omega_n\dot{x} + \omega_n^2 x = \frac{w}{m}K(h)(\Delta x + \eta_2(h)\Delta x^2 + \eta_3(h)\Delta x^3), \quad (1)$$

where x is the direction of the most flexible vibration mode, Δx is the actual chip thickness variation originated in the regenerative effect, that is, it is the difference of the previous and the present cut. The undamped angular natural frequency is ω_n, while ζ is the modal damping ratio, m is the modal mass and w is the chip width. The specific cutting force function is $f(h) = F(h)/w$, and its derivative is the so-called cutting coefficient $K(h) = f'(h)$. The nonlinear coefficients can also be evaluated from the higher derivatives of the specific cutting force as:

$$\eta_2(h) = \frac{f''(h)}{2f'(h)}\left(\frac{1}{m}\right) \quad \text{and} \quad \eta_3(h) = \frac{f'''(h)}{6f'(h)}\left(\frac{1}{m^2}\right). \quad (2)$$

The relative size of the unsafe zone (UZ) between the points HB and B^3 is defined with the ratio (see Fig. 2b for $a_p \sim w$)

$$\Delta w = \frac{w_{B^3} - w_{HB}}{w_{HB}}. \quad (3)$$

The lengthy algebraic derivation in [11] leads to

$$\Delta w(h) = \frac{h^2}{4}\left(\frac{\delta_1(\omega_C)}{\delta_2(\omega_C)}\eta_2^2(h) + 3\eta_3(h)\right) \cong \frac{3}{4}h^2\eta_3(h), \quad (4)$$

where ω_C denotes the chatter frequency. However, the effect of ω_C on the size of the unsafe zone is negligible for realistic machine tool and cutting parameters with the exemption of low cutting speeds where process damping becomes relevant [14,15], or at low chip loads [2]. In other words, the size of the unsafe zone depends mostly on the cubic power of the chip thickness variation in (1), and it is roughly constant all along the lobes whatever vibration (chatter) frequency ω_C occurs in the system.

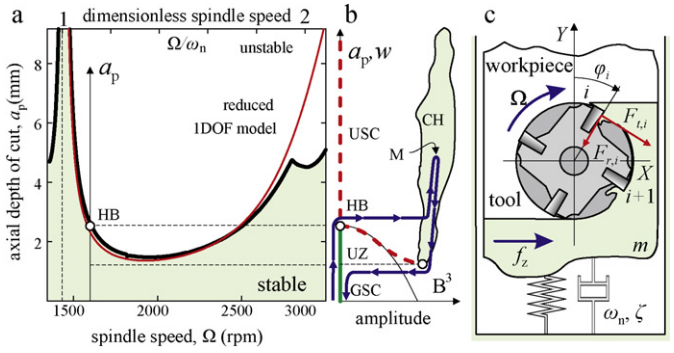

Fig. 2. (a) Stability lobes for reduced 1 DoF model of cutting (red line) and for multi-DoF model of milling (black line). (b) The unsafe zone (UZ) of stationary cutting below the critical depth of cut (HB), above which unstable stationary cutting (USC, dashed red line) occurs; the large amplitude oscillation (chatter, CH) is often chaotic (grey cloud), while the globally stable stationary cutting (GSC, green solid line) appears below the turning point (B^3). HB and B^3 are connected by an unstable "ghost" oscillation (red dashed line) that separates the locally stable stationary cutting and the chatter. Blue solid line refers to the process of measurement along a hysteresis loop (cf. Fig. 3). (c) Sketch of 1 DoF mechanical model.

The real size of the unsafe zone is $\Delta w(h)w_{HB}$, where w_{HB} is the critical chip width at the regenerative loss of cutting stability that is calculated from standard linear theory [12,13].

Substituting (2) into (4), the following second order non-autonomous differential equation is obtained for the cutting coefficient $K = f'$ as function of the chip thickness h:

$$K''(h) - 8\frac{\Delta w(h)}{h^2}K(h) = 0, \quad (5)$$

The corresponding boundary conditions will be discussed later.

3. Cutting force reconstruction

The idea of reconstructing the specific cutting force characteristics $f(h)$ is based on measuring the relative width Δw of the unsafe zone for different chip thickness values h. This can be done by means of the identification of the hysteresis loop with respect to the slow chip width variation along the blue path in Fig. 2b. The substitution of the experimentally identified function $\Delta w(h)$ into the differential equation (5) will lead to the determination of the cutting coefficient function $K(h)$; its integral gives the specific cutting force function $f(h)$.

For small chip thickness values, experiments often show that the hysteresis loop between HB and B^3 in Fig. 2b is independent of the chip thickness h, that is, $\Delta w(h) = \Delta_0$. Then (5) simplifies to an Eulerian-type differential equation with solution

$$K(h) = B_1 h^{\alpha_1} + B_2 h^{\alpha_2}, \quad \alpha_{1,2} = \frac{1}{2}(1 \mp \sqrt{1 + 32\Delta_0}),$$

and the specific cutting force characteristics has the form: $f(h) = C_1 h^{\alpha_1+1} + C_2 h^{\alpha_2+1} + C_3$. If we assume a typical value $\Delta_0 = 5/128 \approx 3.9\%$ for the relative unsafe zone with small chip thickness values [16], then we have $\alpha_1 = -1/4$ and $\alpha_2 = 5/4$. The boundary condition $f(0) = 0$ leads to $C_3 = 0$, while the other 'boundary condition' that the cutting force has a softening characteristics leads to $C_2 = 0$. This means that we obtain the widely used 'three-quarter' rule for the specific cutting force: $f(h) = C_1 h^{3/4}$.

However, high performance cutting uses not just high cutting speeds but also large feed rates where neither the size of the relative unsafe zone is constant nor the cutting force is softening. The experiments of Tobias [3] referred already to slight increase of $\Delta w(h)$ with increasing h, but our experiments in the high performance parameter domain present even a maximum point.

4. Experimental identification of hysteresis effects in milling

In order to measure the hysteresis effect where the unsafe zone takes place, a specially prepared fixture with one degree of freedom flexibility perpendicular to the feed direction (see Fig. 2c) has been used. Full immersion milling of steel (C45) was performed with a cutter having $N = 4$ teeth and diameter $D = 32$ mm. With this arrangement, the tooth pass frequency can be tuned close to the relevant natural frequency to study the first lobe of the stability chart.

The continuous variation of the axial depth of cut a_p was provided by a special 'ramp-like' workpiece (see upper left part of Fig. 3), which was attached to the special fixture in the feed direction. The experimental modal analysis confirmed the existence of the relevant flexible mode in Y direction with $\omega_n = 95.88$Hz, $\zeta = 0.7\%$ and $m = 140.7$ kg apart from other less significant modes in X, Y and Z directions. With the angular position $\varphi_i(t) = t\Omega + 2\pi(i-1)/N$ of the ith tooth (see Fig. 2c), the governing equation for coordinate q in the Y direction is given as:

$$\ddot{q} + 2\zeta\omega_n\dot{q} + \omega_n^2 q = -\frac{a_p}{m}(f_t(h_i)\sin\varphi_i + f_r(h_i)\cos\varphi_i) - \frac{a_p}{m} \times (f_t(h_{i+1})\sin\varphi_{i+1} + f_r(h_{i+1})\cos\varphi_{i+1}) \quad (6)$$

where the instantaneous chip thickness is expressed as $h_i(t) = f_z \sin\varphi_i(t) + (q(t) - q(t-\tau))\cos\varphi_i(t)$ with f_z denoting the feed per

Please cite this article in press as: Stepan G, et al. Identification of cutting force characteristics based on chatter experiments. CIRP Annals - Manufacturing Technology (2011), doi:10.1016/j.cirp.2011.03.100

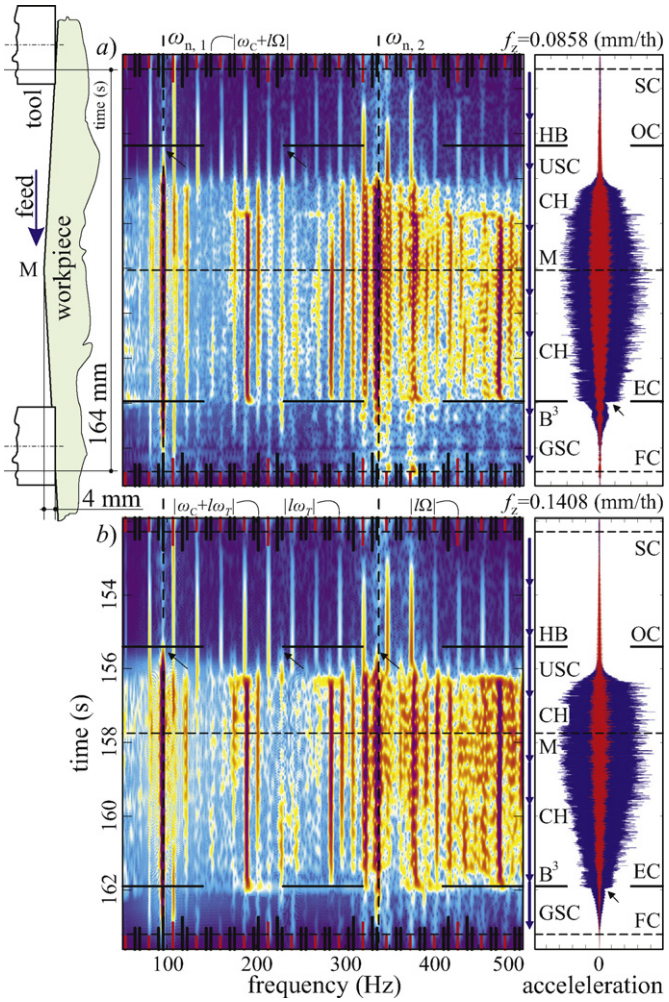

Fig. 3. Samples of the measurement results for the size of the unsafe zone of chatter: time–frequency diagrams of wavelet transforms (left side) of the acceleration (small ~ blue, large ~ red) signals in Y direction and time histories (right side) of accelerations in X (red) and in Y (blue) directions. The vertical time scale is represented by the spatial dimension of the workpiece. The blue path for the increasing/decreasing variation of the depth of cut along the hysteresis loop in Fig. 2b is unfolded to the straight blue line (top-down line with arrows between the wavelet transforms and time histories) with the corresponding critical points identified as follows: SC – start cutting; OC – onset of chatter (HB); M – middle of the workpiece at maximum depth of cut (dashed thin black line); EC – end of chatter (B^3); FC – finish cutting.

tooth. The ratio of the specific tangential and radial force components is the constant $\kappa = f_t/f_r$, so $F_t = f_t a_p$, $F_r = f_r a_p$. Equation (6) is simplified since two teeth are in cut all the time with shift $\pi/2$, i.e., $\varphi_{i+1} = \varphi_i + \pi/2$ (see Fig. 2c).

To have a time independent formulation of (6), we take the time-average of its right-hand-side for the time period $\tau = 2\pi/(N\Omega)$. If the specific tangential cutting force characteristic is represented by a cubic polynomial (see curve C in Fig. 1b)

$$f_t(h) = \rho_1 h + \rho_2 h^2 + \rho_3 h^3 + \cdots, \tag{7}$$

then the governing time-independent differential equation is:

$$\ddot{q} + 2\xi\omega_n\dot{q} + \omega_n^2 q = \frac{a_p}{m}(q_0 + K_1\Delta q + K_2\Delta q^2 + K_3\Delta q^3 + \cdots),$$

where $\Delta q = q(t-\tau) - q(t)$ is the regenerative term with delay τ and coefficients are $q_0 = -f_z\rho_1 - 8f_z^2\rho_2/(3\pi) - 3f_z^3\rho_3/4$, $K_3 = 3\kappa\rho_3/4$, $K_2 = -4\rho_2/(3\pi) - 3f_z\rho_3/4$, $K_1 = \kappa\rho_1 + 8f_z\kappa\rho_2/(3\pi) + 3f_z^2\kappa\rho_3/4$. Introducing the perturbation x by $q(t) = q_0 + x(t)$, we obtain the equation of motion (1), with $\eta_2 = K_2/K_1$, $\eta_3 = K_3/K_1$. The depth of cut a_p and the feed rate f_z take the role of the chip width w and the chip thickness h in (1), while the role of the cutting coefficient K is taken by the coefficient K_1.

By taking care of the edge radius and the highest recommended feed per tooth of the inserts, eight different feeds were selected between $f_z = 0.0583$ and 0.2508mm/tooth. The shots were performed subsequently on a workpiece with symmetric ramps using the fixed spindle speed $\Omega = 1600$ rpm (see Fig. 2a). The steepness of the ramps was designed by means of the predicted stability chart (thick lines in Fig. 2a) using the measured modal parameters and the linear cutting coefficients $K_t = 1495$ N/mm^2, $K_r = 538.7$ N/mm^2. The result was a ramp of 5 mm height in the middle of the workpiece (see upper left side of Fig. 3 and point M with thin horizontal dashed lines in wavelet transforms and time-histories). For safety reasons, the maximum depth of cut was kept at 4mm only.

In Fig. 3, the measured time-histories of acceleration signals are presented together with their wavelet transformations (time-frequency diagrams) in case of two typical shots with different values of feed per tooth. The natural frequencies $\omega_{n,1} = \omega_n$ and $\omega_{n,2}$ in Y appear in the horizontal (frequency) axes of the wavelet transforms presented by vertical dashed lines through the diagrams. Following [17], all the essential frequencies were carefully identified in these wavelet transforms (see inserted vertical lines at top and bottom in Fig. 3): the harmonics of the spindle frequency Ω (short red lines), those of the tooth pass frequency $\omega_T = N\Omega$ (long red lines), the harmonics $|\omega_C + l\Omega|$ and $|\omega_C + l\omega_T|$ of the chatter frequency ω_C by the spindle frequency (short black lines) and by the tooth pass frequency (long black lines) ($l = \pm1, \pm2, \pm3, \ldots$), respectively.

The wavelet transforms in Fig. 3 clearly identify the start (SC) and the finish (FC) of cutting. The onset of chatter (OC) can be identified by means of the traces of the higher harmonics of the chatter frequency in the time-frequency diagrams (see small arrows in the left sides of each panel). The end of chatter (EC) can also be identified by means of the acceleration signals in the time domain: the system 'falls back' to stable stationary cutting from the large-amplitude chatter almost immediately (see arrows in the right side of each panel). Still, this also leaves its clear trace in the time-frequency representation at higher harmonics for the end of chatter (EC). The onset (OC) and the end (EC) of chatter are also marked by thick horizontal dashed lines.

As explained by the blue path of the measurement along the hysteresis loop in Fig. 2b that is unfolded to a top-down straight blue line vertically in time along the spatial dimension of the workpiece in Fig. 3, the experimentally identified (OC) corresponds to the Hopf bifurcation (HB), and (EC) corresponds to the Big Bang bifurcation (B^3). The relative size of the unsafe zone can be calculated from the measurements by (3) as

$$\Delta w(h) \mapsto \Delta a_p(f_z) = \frac{(\overline{OC} - \overline{SC}) - (\overline{FC} - \overline{EC})}{\overline{OC} - \overline{SC}}. \tag{8}$$

5. Force reformulation from the chatter experiments

Based on formula (8), the evaluation of the experimental wavelet transforms for the 8 different feed rates serves the dots in Fig. 4 for the relative size of the unsafe zone depending on feed. This clearly shows a maximum at an extremely large value of 78%, which means that the 'classical' constant unsafe zone of 4% and the corresponding three-quarter rule of cutting force characteristics is not valid at all in case of high-performance milling.

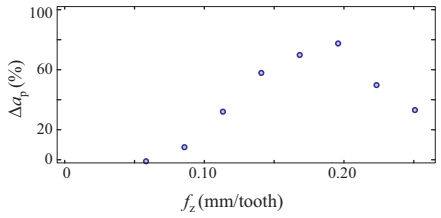

Fig. 4. Measured width of the unsafe zone as function of feed.

Please cite this article in press as: Stepan G, et al. Identification of cutting force characteristics based on chatter experiments. CIRP Annals - Manufacturing Technology (2011), doi:10.1016/j.cirp.2011.03.100

If the approximate function $\Delta a_p = C f_z^2/(1 + b f_z + c f_z^2)$ is fitted to the measured points in Fig. 4 then the solution of the differential equation (5) is a second degree polynomial for the cutting coefficient, and the specific cutting force is just a 3rd degree polynomial as considered in (7) by Tobias [3]. Optimizing the parameters C, b and c and fitted also to the linear stability limit, the parameters $C = 12.51/mm^2$, $b = -11.51/mm$, $c = 53.61/mm^2$ are obtained in Δa_p and the cutting force coefficients in (7) are $\rho_1 = 11.9 \times 10^3$ N/mm^2, $\rho_2 = -161 \times 10^3$ N/mm^3, $\rho_3 = 848 \times 10^3$ N/mm^4.

6. Concluding remarks

Using the wavelet transformation of the measured acceleration signals of chatter induced during milling for different feed rates on workpieces with carefully designed ramps, a simple method was introduced to measure the relative size of the hysteresis loops corresponding to the unsafe cutting parameter zones of regenerative chatter. From fast measurement, formulae can be derived to reconstruct the cutting force characteristics against chip thickness.

If no hysteresis loop is experienced at the stability limit, the linear and shifted linear cutting force characteristics may be used. When the unsafe zone is constant at values of 3–5% then the proposed method leads to the classical power law, and it gives exactly the well-known 3/4 power rule for 3.9%. However, this is not valid for large feed rates. The relative size of the unsafe zone can increase up to 80% as shown in (8) and in Fig. 3 where the strong asymmetry of the onset (OC) and the end (EC) of chatter around the middle point M in the wavelet transforms for the larger feed exists.

When large feed rates lead to a maximum for the measured width of the hysteresis loop, the softening cutting force characteristics may turn to a hardening one at an inflexion. These forces can be described by cubic polynomials well. Further analyses and experiments are needed to check whether the exponential or power expressions of the cutting force can also be fitted to the results of dynamic experiments. However, one important fact has already been confirmed by the measurements: the size of unsafe zone of regenerative chatter has a maximum for increasing feed.

Acknowledgments

This research was partially supported by the Hungarian National Science Foundation under grant OTKA K68910 and by the EU FP7 Dynxperts (260073/FP7-2010-NMP-ICT-FoF).

References

[1] Davies MA, Burns TJ (2001) Thermomechanical Oscillations in Material Flow During High Speed Machining. *Philosophical Transactions of the Royal Society A* 359:821–846.
[2] Jin X, Altintas Y (2011) Slip-Line Field Model of Micro-Cutting Process with Round Tool Edge Effect. *Journal of Materials Processing Technology* 211(3):339–355.
[3] Shi HM, Tobias SA (1984) Theory of Finite Amplitude Machine Tool Instability. *International Journal of Machine Tools Design and Research* 24:45–69.
[4] Endres WJ, Loo M (2002) Modeling Cutting Process Nonlinearity for Stability Analysis—Application to Tooling Selection for Valve-Seat Machining. *Proc. 5th CIRP Workshop*, West Lafayette, USA, .
[5] Taylor FW (1907) On the Art of Cutting Metals. *Transactions of the American Society of Mechanical Engineers* 28:31–350.
[6] Kienzle O (1957) Spezifische schnittkräfte bei der metallbearbeitung. *Werkstattstechnik und Maschinenbau* 47:224–225.
[7] Armarego EJA, Deshpande NP (1989) Computerized Predictive Cutting Models for Forces in End Milling including Eccentricity Effect. *Annals of CIRP* 38(1):45–49.
[8] Wahi P, Chatterjee A (2008) Self-Interrupted Regenerative Metal Cutting in Turning. *International Journal of Non-Linear Mechanics* 43(2):111–123.
[9] Dombovari Z, Barton DAW, Wilson RE, Stepan G (2011) On the Global Dynamics of Chatter in the Orthogonal Cutting Model. *International Journal of Non-Linear Mechanics* 46(1):330–338.
[10] Szalai R, Stepan G, Hogan S (2004) Global Dynamics of Low Immersion High-Speed Milling. *Chaos* 14(4):1069–1077.
[11] Dombovari Z, Wilson R, Stepan G (2008) Estimates of the Bistable Region in Metal Cutting. *Proceedings of the Royal Society A* 464:3255–3271.
[12] Altintas Y, Budak E (1995) Analytical Prediction of Stability Lobes in Milling. *Annals of CIRP* 44(1):357–362.
[13] Stepan G (1989) *Retarded Dynamical Systems*. Longman, London.
[14] Altintas Y, Eynian M, Onozuka H (2008) Identification of Dynamic Cutting Force Coefficients and Chatter Stability with Process Damping. *CIRP Annals—Manufacturing Technology* 57(1):371–374.
[15] Stepan G (2001) Modelling Nonlinear Regenerative Effects in Metal Cutting. *Philosophical Transactions of the Royal Society of London A* 359:739–757.
[16] Kalmar-Nagy T, Stepan G, Moon FC (2001) Subcritical Hopf Bifurcation in the Delay Equation Model for Machine Tool Vibrations. *Nonlinear Dynamics* 26:121–142.
[17] Mann BP, Insperger T, Bayley PV, Stepan G (2003) Stability of Up-Milling and Down-Milling, Part 2: Experimental Verification. *International Journal of Machine Tools & Manufacture* 43:35–40.

Please cite this article in press as: Stepan G, et al. Identification of cutting force characteristics based on chatter experiments. CIRP Annals - Manufacturing Technology (2011), doi:10.1016/j.cirp.2011.03.100